Articles

P61A Mutation in the Factor for Inversion Stimulation Results in a Thermostable Dimeric Intermediate†

Derrick Meinhold, Sarah Boswell,‡ and Wilfredo Colón*

Department of Chemistry and Chemical Biology, Rensselaer Polytechnic Institute, 110 Eighth Street, Troy, New York 12180

Received April 6, 2005; Revised Manuscript Received September 13, 2005

ABSTRACT: The factor for inversion stimulation (FIS) is a homodimeric DNA-binding protein found in enteric bacteria. FIS consists of 98 residues and self-assembles into an entwined dimer containing a flexible and mostly disordered N-terminus followed by four α-helices. Proline 61, which is 100% conserved in FIS homologues, is located at the center of helix B, and its substitution for alanine (P61A) was previously shown to result in nonuniform stabilization of the protein, leading to the appearance of a marginally populated dimeric intermediate in urea denaturation equilibrium studies. Here we show that, in contrast to WT FIS, the thermal denaturation of P61A FIS was incomplete and yielded a transition curve that was independent of FIS concentration, suggesting the presence of a dimeric intermediate at 90 °C. In the presence of urea, the thermal denaturation of P61A FIS became concentration dependent, consistent with the denaturation of the dimeric intermediate. The existence of a thermostable dimeric intermediate of P61A FIS was further confirmed by glutaraldehyde cross-linking experiments at 95 °C. Urea denaturation experiments at 90 °C revealed a cooperative transition, indicating that the dimeric intermediate of P61A FIS has a solvent-protected hydrophobic core. P61A FIS, unlike the WT protein, was found to be resistant to denaturation by low pH, but its thermal denaturation at pH 3.5 revealed a biphasic transition, providing clues about the structure of the dimeric intermediate. From a functional perspective, it is plausible that the full conservation of proline 61 in FIS may serve to limit the stability and proteolytic resistance of this highly regulated transcription factor.

The factor for inversion stimulation (FIS)[1] is a dimeric DNA-binding protein found in enteric bacteria where it is involved in a number of expression regulation functions, including site-specific DNA inversion (*1*, *2*) as well as the regulation of its own transcription (*3*, *4*). The positively charged C-terminus is involved in DNA binding, and the N-terminal helix binds Hin and Gin recombinases to stimulate DNA inversion (*5*). FIS is a good model for folding and stability studies of dimeric proteins because it is relatively small (98 AA per chain), lacks disulfide bonds, and unfolds reversibly (*6*). The main dimerization interface involves the interaction of helix B from one subunit with helices A and B of another FIS subunit. At position 61, located in the middle of helix B, there is a highly conserved proline residue that appears to support a 20° kink in the helix. Interestingly, a proline 61 to alanine (P61A) mutation has been found to cause only slight changes in the structure of FIS, and the kink angle in helix B decreases modestly from 20° to 16° (Figure 1) (*7*). In addition, the mutation introduces a hydrogen bond between the backbone amide of alanine 61 and the side chain carboxyl group of glutamic acid 57 (*7*). Since proline 61 is 100% conserved in all strains of enteric bacteria in which FIS has been identified (*8*), there may be a structural or functional reason for the presence of a proline in the middle of the protein's main helix, especially

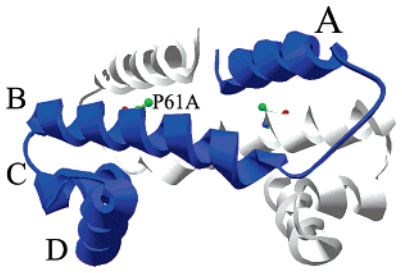

FIGURE 1: X-ray crystal structure of P61A FIS (PDB file 1FIP) (*7*). The first 25 residues of each monomer in both P61A and the WT are highly mobile and therefore are not resolved by the crystal structure. The four α-helices in the protein are labeled A through D. This figure was prepared using the program Deepview (*21*).

† This work was supported by grants from the National Science Foundation (NSF MCB-9984913 to W.C.).

* To whom correspondence should be addressed. E-mail: colonw@rpi.edu. Phone: (518) 276-2515. Fax: (518) 276-4887.

‡ Current address: Cutaneous Biology Research Center, Massachussets General Hospital, 13th Street, Building 149, Charlestown, MA 02129.

[1] Abbreviations: AA, amino acid; CD, circular dichroism; far-UV, far-ultraviolet; FIS, factor for inversion stimulation; K_U, equilibrium constant for unfolding; P61A, proline to alanine mutation at position 61; PB, phosphate buffer; SDS−PAGE, sodium dodecyl sulfate−polyacrylamide gel electrophoresis; T_m, midpoint of thermal denaturation; WT, wild type.

10.1021/bi050640k CCC: $30.25 © 2005 American Chemical Society
Published on Web 10/21/2005

since proline residues in helices are highly destabilizing and more commonly found toward the end of the helix (*9*).

Recently, we showed that the P61A mutation in FIS increased the overall protein stability by about 4 kcal/mol (*10*). Interestingly, the urea-induced denaturation transition of P61A FIS appeared to be two state like, but the slope of the transition (*m*-value) decreased with increasing protein concentration, suggesting that the denaturation mechanism was not two state. Global fitting analysis of the data was consistent with a three-state denaturation mechanism involving the marginal population of a dimeric intermediate (*10*). The P61A mutation appears to introduce a dimeric intermediate by stabilizing the dimeric core (helices A and B) to a greater extent than the C-terminal subdomain (helices C and D), in part due to weakening of the salt bridge interactions that help to connect the B-helix to the C- and D-helices. Consequently, the P61A FIS mutation resulted in greater proteolytic susceptibility of the C-terminal region while rendering the dimeric core (helices A and B) nearly resistant to cleavage by trypsin (*10*). On the basis of this and the fact that the C- and D-helices are mainly involved in intramolecular interactions (Figure 1), we proposed that the dimeric intermediate might involve a partially unfolded C-terminus. Thus, in contrast to the WT protein, where the stability of all the helices is interdependent, resulting in a cooperative urea-induced denaturation transition, in the case of P61A FIS, the mutation somewhat compromised the denaturation cooperativity by overstabilizing the dimeric core relative to the C-terminus.

On the basis of the results of our previous urea denaturation and limited proteolysis studies of P61A FIS (*10*), we were interested in comparing the thermal denaturation mechanism of WT and P61A FIS. Our preliminary data showed that a complete denaturation transition for WT FIS at a concentration of 8.9 μM requires at least 80 °C, raising the question of how high a temperature would be necessary to denature the much more stable P61A FIS and whether we would observe a breakdown in the denaturation cooperativity as was observed in the urea denaturation studies. Here we show that, in contrast to WT FIS, the thermal denaturation of P61A yields a less cooperative and incomplete denaturation curve that is independent of FIS concentration, suggesting the presence of a dimeric intermediate that is stable at 90 °C. The presence of the dimeric intermediate was confirmed using several complementary methods. These results suggest that FIS is an inherently thermally stable protein with a stability that is limited, perhaps for functional reason, by the presence of a proline in the middle of its main helix.

MATERIALS AND METHODS

Protein Expression, Purification, and Preparation. The P61A FIS mutant expression plasmid was constructed and sequenced as previously described with a two-step megaprimer PCR method (*10*). WT and P61A FIS were overexpressed in *Escherichia coli* and purified using a SP-Sepharose cation-exchange column followed by desalting precipitation, resulting in 95% pure FIS according to sodium dodecyl sulfate−polyacrylamide gel electrophoresis (SDS−PAGE). The concentration of FIS was determined using UV spectroscopy and an extinction coefficient of 6340 and 6370 M^{-1} cm^{-1} for WT and P61A FIS, respectively (*10*). All experiments were performed in 10 mM phosphate buffer (PB) at pH 7.4 with 0.1 M NaCl, except for the pH denaturation experiments and low-pH thermal denaturations for which conditions are described below.

Circular Dichroism Studies of FIS. Circular dichroism (CD) experiments were performed with an OLIS CD instrument (Bogart, GA) equipped with a dual beam optical system. The temperature was adjusted with a Julabo water bath (Allentown, PA) and was controlled automatically with the OLIS thermal control software. The recorded temperatures were calibrated by correlating the cell-holder temperature with the actual temperature of the sample in the cell. Optimal equilibration times for thermal denaturations were determined on the basis of the volume of the cell used. At 8.9 μM FIS, a cell with a 2 mm path length was used with an equilibration time of 4 min, while at 1.8 μM FIS a cell with a 1 cm path length was used and 9 min of equilibration time was required. The equilibration times that are reported here were proven sufficient by observing identical data when equilibrating for longer times (data not shown). Data consistency between cell size and type was verified by testing the thermal denaturation at both protein concentrations (8.9 and 1.8 μM) in the 1 cm cell. Reversibility of the thermal denaturation was verified by collecting data while heating the protein to 95 °C and then while cooling back to 15 °C, as well as by consecutive thermal denaturations on the same sample. Reversible transitions recovered about 95% of the original signal in the absence of urea and showed the same transition midpoint as seen in the original denaturation experiment (data not shown). Thermal denaturations in the presence of urea recovered slightly less signal upon refolding than in the absence of urea but showed similar curves and T_ms as the original unfolding curve.

Equilibrium thermal denaturation was monitored with CD at 222 nm to follow the secondary structure and at 255 nm for baseline correction. All CD thermal denaturations were performed at 8.9 or 1.8 μM FIS. For each thermal denaturation experiment, one WT or P61A FIS sample was prepared in 10 mM PB and 0.1 M NaCl (pH 7.4) and then heated, equilibrated, and scanned at temperatures between 10 and 95 °C. Thermal denaturation experiments in the presence of urea were performed at 1.8 and 8.9 μM FIS in the same manner as described above, and low-pH samples were adjusted with HCl. We used reverse-phase HPLC and mass spectrometry to determine whether samples exposed to urea at high temperature had undergone chemical modification due to the decomposition of urea. Reverse-phase HPLC showed no effect on peak retention time when the protein was incubated in 2 M urea for WT and 2 or 4 M urea for P61A at 80° C for 5 min and then raised to 90 °C for 5 min. However, mass spectrometry revealed an additional smaller peak with a mass consistent with carbamylation. Fortunately, the modification of FIS did not significantly affect the reversibility of the thermal denaturation transition. Urea-induced equilibrium denaturations at 90 °C were performed at 8.9 μM FIS and were monitored with CD. Individual samples were prepared and equilibrated to 80 °C for 10 min and then placed in the instrument, capped, and equilibrated to 90 °C for 10 min. Urea concentrations for all experiments were determined by measuring the refractive index with an

Abbe refractometer after each scan. Acid-induced denaturations were performed in 10 mM PB. The monobasic and diabasic ratios were adjusted for individual samples such that a minimum concentration of HCl (<0.02 M) was needed to adjust to the desired pH of each sample. Normalization of thermal denaturation data in Figures 2 and 3 was done according to the expression: (signal − $\text{signal}_{\text{folded}}$)/($\Delta\text{signal}_{\text{WT}}$), where $\text{signal}_{\text{folded}}$ represents the signal of the folded protein at 20 °C and $\Delta\text{signal}_{\text{WT}}$ represents the difference in signal between the folded and unfolded ($\text{signal}_{\text{unfolded}}$ − $\text{signal}_{\text{folded}}$) WT FIS protein. By using this normalization scheme, the *y*-axis is scaled on the basis of the normalization of the WT data from zero (completely folded) to one (completely unfolded), and it allows direct comparison of the percentage of unfolded P61A and WT FIS. The urea denaturation curve in Figure 5 was internally normalized from 0% to 100% as follows: (signal − $\text{signal}_{\text{folded}}$)/($\text{signal}_{\text{unfolded}}$ − $\text{signal}_{\text{folded}}$). The data in Figure 6 were internally normalized relative to the native signal using the equation (signal − $\text{signal}_{\text{folded}}$)/($\text{signal}_{\text{folded}}$) to preserve the raw data and allow comparison between the different transitions.

Glutaraldehyde Cross-Linking (GCL). Protein samples (8.9 μM) were incubated for at least 10 min at the desired temperature and urea concentration before glutaraldehyde was added to a final concentration of 0.5% (v/v). After 1 min of cross-linking, the reaction was quenched with a final concentration of 0.05 M $NaBH_4$ and then precipitated with deoxycholic acid and trichloroacetic acid at final concentrations of 0.1% (w/v) and 5% (w/v), respectively. The samples were centrifuged at 9000*g* for 10 min, and the protein pellet was resuspended in 40 μL of 4% SDS−PAGE sample buffer [0.125 M tris(hydroxymethyl)aminomethane hydrochloride, 4% SDS, 20% v/v glycerol, 0.02% bromophenol blue, pH 6.8]. The samples were loaded onto a 16% glycine SDS−PAGE gel. The gels were photographed and quantified using the DigiDoc image analysis software from Alpha Innotech (San Leandro, CA). The minor bands that appear above the cross-linked dimer were not considered in the analysis of the data.

Data Analysis. All of the thermal denaturation data were normalized according to relative degree of native signal loss, either internally or with respect to the WT FIS signal loss as described above. Relative signal loss normalization was necessary for comparison of P61A and WT FIS because they lose different degrees of total native signal during unfolding. Normalization in this manner preserves the baseline slopes and does not require a defined post-transition baseline slope, which is lacking for the P61A transitions in Figure 2B.

Data fitting was done using KaleidaGraph software version 3.51 (Synergy Software) except when stated otherwise. For all two-state ($N_2 \leftrightarrows 2U$) fits, the instrument signal (Y) was fitted to the equation:

$$Y = Y_N(1 - F_U) + Y_U F_U \quad (1)$$

where Y is equal to the fraction unfolded (F_U) plus fraction native ($1 - F_U$) multiplied by the native (Y_N) and unfolded (Y_U) signals, which vary linearly with temperature or urea concentration. To obtain the thermodynamic parameters, F_U is defined in terms of the equilibrium constant for unfolding (K_U) and the total monomer concentration (P_t) by combining the equations $K_U = [U]^2/[N_2]$, $P_t = 2[N_2] + [U]$, and $F_U = [U]/P_t$ to obtain the equation (*11*):

$$F_U = \frac{-K_U + \sqrt{K_U^2 + 8K_U P_t}}{4P_t} \quad (2)$$

The equilibrium constant for thermal denaturation may be expressed (*12*−*14*) as

$$K_U(T) = P_t \exp\left[\frac{-\Delta H(T_m)}{R}\left(\frac{1}{T} - \frac{1}{T_m}\right) + \frac{\Delta C_p}{R}\left(\ln\frac{T}{T_m} + \frac{T_m}{T} - 1\right)\right] \quad (3)$$

where ΔH and ΔC_p are the changes in enthalpy and heat capacity, respectively, between the folded and unfolded states at the T_m and R is the gas constant [$R = 0.0019872$ kcal/(mol·K)]. The P_t term in eq 3 serves to counterbalance the protein concentration-dependent T_m, thereby yielding, as theoretically expected, the same equilibrium constant (K_U) at different protein concentrations. ΔC_p is held constant in the equation, but ΔH is mainly dictated by the transition slope and, therefore, is also protein concentration independent for a simple $N_2 \leftrightarrows 2U$ model. The parameters (T_m and ΔH) derived from fits to the WT FIS data at 0 and 2 M urea and two protein concentrations were substituted into eq 3 and yielded calculated K_{eq} vs T curves that were independent of protein concentration throughout the transition region (data not shown).

Urea denaturation at 90 °C was analyzed on the basis of the two-state transition $I_2 \leftrightarrows 2U$ (*10*) with a K_U defined as

$$K_U = \exp\left(\frac{-\Delta G_{H_2O} + mD}{RT}\right) \quad (4)$$

where ΔG_{H_2O} is the protein stability in the absence of denaturant and D is the denaturant molar concentration. The m-value is the urea dependence of the stability which correlates with the amount of buried surface area that becomes exposed upon unfolding (*15*).

The pH denaturation curve (Figure 6A) was analyzed by fitting it to the equation:

$$\text{signal} = \frac{\alpha_N + \beta_N(\text{pH}) + (\alpha_D + \beta_D(\text{pH})) \times 10^{-M_{eq}(\text{pH}-\text{mp})}}{1 + 10^{-M_{eq}(\text{pH}-\text{mp})}} \quad (5)$$

where mp is the midpoint of the transition, M_{eq} is the number of protons that bind during unfolding, and α and β represent the y-intercept and slope, respectively, for the signals of the native (N) and denatured (D) states.

The change in heat capacity upon unfolding of P61A and WT FIS was estimated for use as a constant in eq 3 to fit the thermal denaturation data. The ΔC_p was estimated by global fitting urea denaturation curves at eight temperatures between 280 and 330 K using eqs 2 and 4 and thermal denaturation curves with fixed amounts of urea up to 2.5 and 5 M for WT and P61A, respectively. The thermal denaturation curves in the global optimization were fit with eq 2 and an altered version of eq 3 which fits to T_g rather than T_m, where T_g is the temperature at which $\Delta G = 0$. A

global fit was obtained by optimizing all parameters of the individual curve fits to not only fit the unfolding traces but also fit their ΔG values with the Gibbs−Helmholtz protein stability curve. Thermal denaturations contributed to the protein stability curve by supplying ΔG values above 350 K at each urea concentration studied, whereas the urea denaturation curves contributed to the protein stability curve by providing ΔG values from 280 to 330 K in the absence of denaturant. In addition, the ΔG values from the urea denaturations were extrapolated to the exact urea concentrations that were used in the various thermal denaturations, thereby allowing for a protein stability curve fit at each urea concentration. Fitting was done using the solver function of Microsoft Excel by minimizing the sum of squared errors of the fits to the urea and thermal denaturation data and the sum of squared errors of the protein stability curve fit to the ΔG values. Error was minimized by allowing the program to vary all the fitting parameters to the individual fits, as well as the parameters defining the protein stability curve. The result was a set of ΔG versus temperature curves at various urea concentrations that nicely fit to the determined and extrapolated ΔG values while accurately fitting to the individual urea and thermal denaturation transitions.

RESULTS

Thermal Denaturation of FIS. P61A and WT FIS display characteristic α-helical far-UV CD spectra with similar magnitudes of signal in the folded state (Figure 2A). In contrast, the thermally unfolded state of the P61A FIS at 90 °C retains significantly more structure than that of WT FIS (Figure 2A). The fraction of residual ellipticity of unfolded WT and P61A FIS, relative to the native signal at 222 nm and 20 °C, is 45.2 ± 3.4 and 55.5 ± 6.2, respectively. This suggests not only that FIS is incompletely unfolded by thermal denaturation but also that P61A FIS retains more helical structure than the WT protein at 90 °C. Thermal denaturation experiments show a concerted two-state transition for WT FIS, whereas the P61A FIS transition is less cooperative and does not come to completion within the temperature range of the experiment (Figure 2B). The significant decrease in cooperativity of the P61A FIS transition hints at the presence of a denaturation intermediate. Figure 2 also shows that the P61A mutation significantly increases the resistance of FIS to thermal denaturation, resulting in a transition that is about 15−20 °C higher than that of WT. Interestingly, in contrast to that of WT FIS, the transition of P61A FIS is not dependent on protein concentration (Figure 2B). WT FIS exhibits T_ms of 58 and 63 °C at protein concentrations of 1.8 and 8.9 μM, respectively, with corresponding ΔH values of 53.1 and 53.0 kcal/mol (Table 1). The lack of a concentration-dependent transition for P61A FIS suggests the presence of a thermostable dimeric intermediate at 90 °C.

Thermal Denaturation in the Presence of Urea. Thermal denaturation of FIS samples in the presence of urea was used to destabilize the apparent P61A dimer that exists at 90 °C in an attempt to restore the concentration dependence expected for a $N_2 \leftrightarrows 2U$ transition. The urea concentrations chosen were 2 and 4 M urea for WT and P61A FIS, respectively, since they are the highest urea concentrations that do not cause loss of secondary structure at 20 °C at the protein concentrations studied here (Figure 3A) (*10*) and represent similar conditions with respect to the different stabilities of WT and P61A FIS. As expected, the WT thermal denaturation transition in the presence of 2 M urea remains dependent on protein concentration, exhibiting T_ms of 39 and 45 °C for 1.8 and 8.9 μM FIS, respectively (Figure

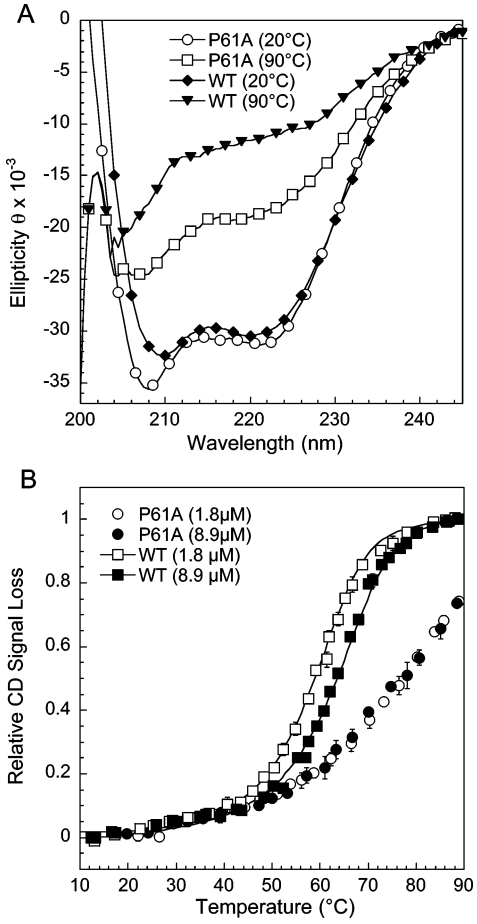

FIGURE 2: (A) Far-UV wavelength scans of P61A and WT FIS at 20 and 90 °C. All protein concentrations were 8.9 μM. The units of ellipticity, θ, are deg·cm^2. (B) Temperature-induced denaturation of P61A FIS at 8.9 and 1.8 μM and WT FIS at 8.9 and 1.8 μM measured by far-UV CD. Error bars are averaged from at least three different data sets. The solid lines represent a two-state dimer to monomer unfolding curve fit as described in Materials and Methods.

Table 1: Thermodynamic Parameters from Thermal Denaturation Fits Using a Two-State $N_2 \leftrightarrows 2U$ Model[a]

protein	[urea]	$[P_t]$ (μM)	ΔH (kcal/mol)	T_m (°C)	ΔG (kcal/mol)[b]
WT	0	1.8	53.1 ± 3.4	58.1 ± 0.5	11.3 ± 0.5
WT	0	8.9	53.0 ± 1.3	63.2 ± 0.2	10.4 ± 0.2
WT	2	1.8	54.9 ± 3.7	39.2 ± 0.2	10.6 ± 0.2
WT	2	8.9	53.9 ± 6.8	45.5 ± 0.9	10.4 ± 0.7
P61A	4	1.8	36.0 ± 1.3	52.2 ± 0.2	10.8 ± 0.1
P61A	4	8.9	21.4 ± 1.5	56.7 ± 0.6	8.5 ± 0.2

[a] Estimated ΔC_p values were used to fit the data: 1.1 kcal/(mol·K) for WT in the absence of urea and 0.8 and 0.3 kcal/mol in the presence of urea for WT and P61A, respectively. These ΔC_p values were estimated from the temperature dependence of the ΔG of unfolding calculated from urea and thermal denaturation at various temperatures and urea concentrations (see Materials and Methods). Errors are equal to one standard deviation derived from at least three separate experiments. [b] The ΔG at 20 °C was calculated by substituting the curve fit parameters ΔH and T_m into eq 3 and then converting the equilibrium constant into ΔG. Error values were calculated by propagating the errors of the T_m and ΔH.

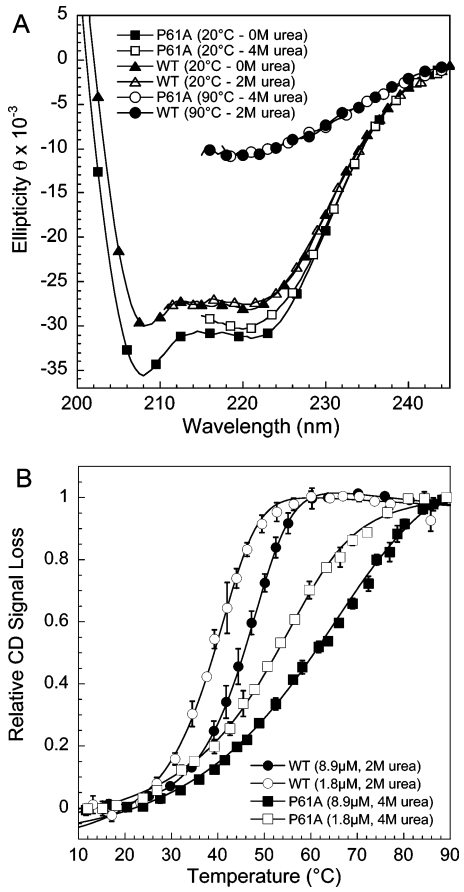

FIGURE 3: (A) Far-UV wavelength scans of P61A and WT FIS at 20 °C and in the presence of 4 M urea (P61A) and 2 M urea (WT) at 20 and 90 °C. All protein concentrations were 8.9 μM. The units of ellipticity, θ, are deg·cm^2. (B) Temperature-induced denaturation of P61A and WT FIS in 4 and 2 M urea, respectively, monitored by far-UV CD. P61A was monitored at 8.9 and 1.8 μM in addition to WT FIS at the same concentrations, 8.9 and 1.8 μM. Error bars are averaged from at least three different data sets. Solid lines represent a fit to eqs 2 and 3 to obtain the thermodynamic parameter shown in Table 1. Since panel A shows that both WT and P61A FIS unfold to the same extent at 90 °C, to obtain a reliable fit of the P61A data, the well-defined post-transition baseline of WT FIS was used to define the post-transition baseline of P61A FIS.

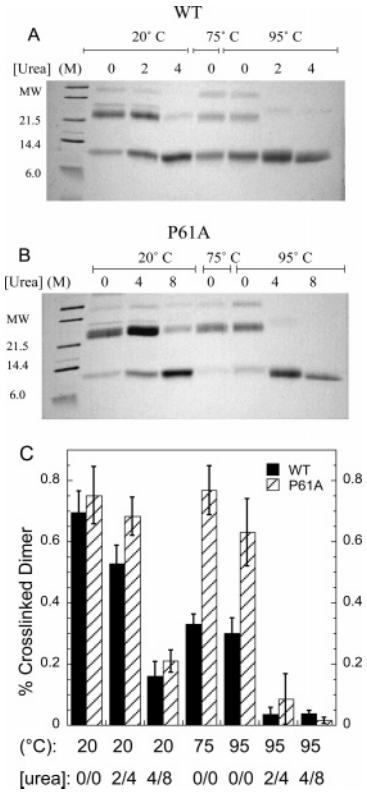

FIGURE 4: P61A (A) and WT (B) FIS at various temperatures and urea concentrations were cross-linked with glutaraldehyde and analyzed by SDS−PAGE. Separate samples were equilibrated at 20, 75, and 95 °C in the presence of 0, 2, 4, and 8 M urea, as indicated above the gels. Panel C shows the average amount of cross-linked dimer along with the standard deviations determined from four independent experiments.

3B). At 4 M urea, the protein concentration dependence becomes evident in the thermal denaturation of P61A FIS, with resulting T_ms of 52 and 57 °C at protein concentrations of 1.8 and 8.9 μM, respectively (Table 1). Despite the change to a concentration-dependent transition, the P61A FIS variant still displays a lower ΔH than WT FIS at both protein concentrations studied. Additionally, there is a significant difference in the ΔH's, 36 (at 1.8 μM) and 21 (at 8.9 μM) kcal/mol, between the two concentrations of P61A studied (Table 1). Such a change in ΔH's at different protein concentrations is inconsistent with a two-state denaturation mechanism and with the low ΔC_p estimated [less than 1 kcal/(mol·deg); data not shown] for P61A FIS. Moreover, as seen for WT FIS in the 0 M urea thermal denaturation experiments, a shift in ΔH is not seen for WT FIS incubated in 2 M urea, where the data show similar ΔH values of 55 and 54 kcal/mol at 1.8 and 8.9 μM, respectively. Therefore, the difference in ΔH values for P61A is suggestive of the presence of an intermediate not present in WT FIS (*10*, *16*). The ΔG values for WT FIS at 0 and 2 M urea show no significant difference at different protein concentrations. This is expected from a protein that follows a two-state denaturation pathway. In contrast, the ΔG of P61A FIS varies significantly with protein concentration, indicative of non-two-state unfolding.

Glutaraldehyde Cross-Linking Traps the Dimeric P61A FIS Intermediate at 90 °C. Glutaraldehyde cross-linking (GCL) was used to trap the dimeric structure of WT and P61A FIS at various temperatures (Figure 4). The efficiency of GCL varies for different proteins and is dependent on several factors, including the number of lysine residues and their location within the protein. In the case of FIS, GCL is a fairly good cross-linker although it fails to trap the entire population of WT and P61A FIS dimer at 20 °C in the absence of urea. At 20 °C, GCL traps about 70% of the WT dimer (Figure 4A,C), and this number decreases modestly at 2 M urea. However, WT FIS is effectively reduced to almost all monomer by 4 M urea, consistent with previous equilibrium urea denaturation experiments (*6*). WT FIS unfolds mainly to the monomer at 75 °C, as can be seen by the drastic reduction of the dimeric band (Figure 4A). At 95 °C, only about 30% of the total dimeric WT band shows on the gel and is virtually 100% reduced to monomer with the addition of 2 and 4 M urea. The results of the GCL in the presence of urea support the validity of the cross-linking experiment because they are quite consistent with the urea denaturation of WT FIS monitored by far-UV CD (*6*). WT FIS retains all native secondary structure in 2 M urea at 20 °C and is unfolded at 4 M urea. When FIS becomes unfolded to the monomeric state, it is clearly not cross-linked by

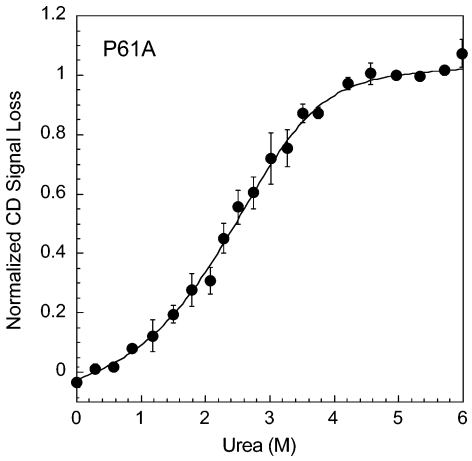

FIGURE 5: Urea-induced denaturation of P61A FIS at 90 °C monitored by far-UV CD. Error bars are averaged from at least three different data sets. The solid line represents a two-state dimer to monomer curve fit. The parameters ΔG, 11.6 ± 0.4 kcal/mol, and *m*-value, 1.4 ± 0.2, were extracted from the fit, and error values were determined directly from the error-weighted curve fit.

glutaraldehyde at 20 or 95 °C. The average percentages of dimer present under the various conditions were analyzed using a gel imaging system, and the result is shown as a bar graph in Figure 4C. The minor band seen above the cross-linked dimer runs between the 31 and 36 kDa MW markers and appears to arise from the undesirable cross-linking of a FIS dimer and monomer molecule. Therefore, this band was omitted from the calculation of the percent of cross-linked dimer shown in Figure 4C.

Most of the P61A FIS dimer present at 20 °C becomes cross-linked, and the reaction efficiency is not altered significantly by the addition of 4 M urea. However, addition of 8 M urea reduces most of the P61A FIS dimer to monomer, in agreement with our previous data showing nearly complete loss of P61A secondary structure at 8 M urea (*10*). Virtually no change can be noted in the cross-linked population of P61A FIS between 20 and 75 °C at 0 M urea. Even at 95 °C, most of the P61A FIS that was cross-linked at 20 °C remains cross-linked as a dimer. Addition of 4 and 8 M urea to the P61A FIS sample at 95 °C shifts the dimeric band almost completely to the monomer, consistent with the extensive dissociation and unfolding of the protein under these conditions. Thus, the cross-linking experiments strongly suggest that the P61A mutation introduces a thermostable dimeric intermediate state that becomes populated at high temperature in the absence of urea.

Urea Denaturation of P61A FIS at 90 °C. The appearance of a dimeric intermediate at 90 °C prompted us to further investigate its stability. Therefore, we carried out urea denaturation experiments at 90 °C to probe for the presence of a cooperative denaturation transition, which would indicate the presence of a solvent-protected hydrophobic core in the P61A FIS thermostable dimer. As expected, no cooperative denaturation transition at 90 °C was observed for WT FIS (data not shown); however, P61A FIS exhibited a cooperative two-state transition (Figure 5). Unfortunately, we were not able to perform this experiment at different protein concentrations since concentrations greater than 8.9 μM resulted in aggregation at 90 °C, and lower concentrations yielded insufficient signal to collect reliable data. For these same reasons it was not feasible to reliably test the reversibility of this transition. Even though P61A FIS displays high reversibility in the presence of urea when heated to 90 °C for 30 min and then promptly cooled (data not shown), this does not exclude the possibility that irreversibly misfolded and aggregated FIS slowly accumulates when the protein is left at high temperatures for hours. Therefore, although we can only be partially confident of its reversibility, the P61A FIS data were fit to the two-state transition $I_2 \leftrightharpoons 2U$ model to obtain an estimate of the stability of the P61A FIS intermediate at 90 °C (Figure 5). The two-state fit yielded values of 11.6 and 1.4 kcal·mol^{-1}·M^{-1} for the ΔG and *m*-value, respectively. These values are roughly 65% of the ΔG and *m*-values determined for P61A FIS at 20 °C (*10*).

P61A FIS Is Resistant to Acid-Induced Denaturation. The original impetus for investigating the pH stability of WT and P61A FIS was to carry out thermal denaturations at various pHs, which usually shifts the T_m and changes ΔH and, in turn, can be used to determine ΔC_p (*17*). However, the pH-induced denaturation study revealed some interesting differences between P61A and WT FIS that may help to understand the thermal denaturation mechanism of P61A FIS and the role of salt bridge interactions in the stabilization of the thermostable dimeric intermediate. The acid-induced denaturation experiments were done in the absence of NaCl because mild concentrations of the chloride ion (0.1 M) are generally found to stimulate the formation of molten globules at low pH (*18*, *19*). In fact, WT FIS exhibits only a marginal loss of secondary structure (<10%) at pH 2 and 0.1 M NaCl (data not shown), whereas in the presence of <0.05 M NaCl roughly 60% of the folded signal of WT FIS is lost at pH 2 (Figure 6A). The pH denaturation of WT had a transition midpoint of about pH 3.2 and was found to involve the binding of 2.3 (M_{eq}) protons per monomer upon unfolding. The M_{eq} value of 2.3 for WT FIS suggests that two or three negatively charged residues may contribute significantly to the stability of WT FIS through the formation of salt bridges. In striking contrast to the pH stability of WT FIS, the P61A FIS mutant renders the protein largely pH resistant, although there are some changes in CD signal that suggest minor conformational shifts (Figure 6A).

Thermal Denaturation at Low pH. If P61A FIS is destabilized, but not unfolded, by acidic pH at 20 °C, then its thermal denaturation at low pH should reflect the combined destabilizing effect of low pH and high temperature. Thermal denaturation experiments were carried out at pH 3.5 to ensure that WT FIS started in the folded state and to prevent potential formation of the molten globule state at lower pH. Analogous to the effect of 2 M urea on the stability and thermal denaturation transition of WT FIS (Figure 3), the thermal denaturation at pH 3.5 revealed a cooperative transition with a reduction in the T_m of about 12 °C (Figure 6B). Surprisingly, the thermal denaturation of P61A FIS at pH 3.5 resulted in the appearance of a biphasic denaturation transition (Figure 6B), with the first transition closely overlaying that of the single WT FIS transition and a second transition that, perhaps coincidently, seems to overlay the transition of P61A FIS at pH 7.4 (Figure 2). The first transition is clearly pH dependent since this transition was not present at pH 7.4; however, the second transition appears to be less affected by low pH. When the experiment was carried out at a higher protein concentration, the first transition did not shift, thereby supporting the hypothesis

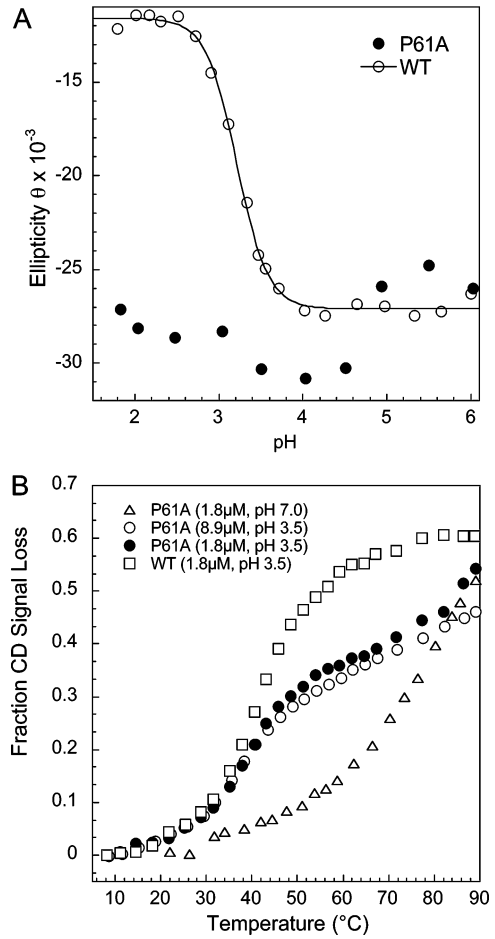

FIGURE 6: (A) pH denaturation of P61A and WT FIS at 1.8 μM monitored by far-UV CD at 20 °C. (B) The thermal denaturation of P61A FIS at pH 3.5 using 1.8 and 8.9 μM FIS and 1.8 μM WT FIS is plotted with the pH 7.4 thermal denaturation of P61A FIS at 8.9 μM. The solid lines were obtained by fitting the data using eq 5.

that this transition corresponds to the nativelike P61A FIS dimer unfolding to a dimeric intermediate (Figure 6B). The concentration dependence of the second P61A FIS transition can be noticed above 70 °C, where at 8.9 μM the transition appears to have shifted to the right and out of the temperature range where it can be seen. Thus, these results suggest that low pH is able to selectively destabilize a region of P61A FIS involved mainly in intramolecular interactions while not significantly affecting the stability of the thermostable dimeric intermediate.

DISCUSSION

Thermostable Dimeric Intermediate of P61A FIS. A summary of the results from the denaturation of WT and P61A FIS using urea, temperature, and low pH is shown in Table 2. As expected for a two-state equilibrium mechanism, the denaturation of WT FIS is characterized by a single cooperative concentration-dependent transition, regardless of the denaturation method (*6*). This indicates that the stability of the dimer core (helices A and B) and the DNA-binding subdomain (helices C and D) are coupled, such that the disruption of one automatically results in the disorder of the other. In the case of P61A FIS, the denaturation is clearly not two state. This is most evident in the thermal denaturation experiments, where, at pH 7.4, the transition not only is concentration independent but also lacks a post-transition baseline and fails to reach the signal expected for unfolded WT FIS (Figure 2). Interestingly, at 20 °C the secondary structure of P61A FIS is not significantly affected by acidic pH (Figure 6), which is an indication that the stabilizing effect of the P61A mutation is greater than the potentially destabilizing effect of low pH. Thus, in contrast to WT FIS, the effect of urea, temperature, and pH denaturation yields drastically different results (Table 2), confirming the more complex denaturation mechanism of P61A FIS.

The concentration independence of the P61A thermal denaturation (Figure 2), the presence of a dimer at 95 °C, as shown by glutaraldehyde cross-linking (Figure 4), and the introduction of concentration dependence in the thermal denaturation transition in the presence of urea (Figure 3) support a denaturation mechanism involving a dimeric intermediate. It is worth noting that the transition slope of P61A (Figures 2 and 3) is significantly less than that of WT FIS, consistent with a lower ΔH of unfolding (Table 1) and the presence of a significant degree of structure at high temperatures. Further support for the presence of a dimeric intermediate comes from the biphasic transition of the thermal denaturation experiments performed at low pH. The intermediate populated in this transition is dimeric, as suggested by the concentration independence of the first transition and the concentration dependence of the second transition (Figure 6B).

The Dimeric Intermediate Appears To Have a Disrupted C-Terminus. Despite the appearance of a two-state transition for P61A FIS upon urea denaturation, our previous studies showed that there was a decrease in the *m*-value of the transitions with increasing P61A FIS concentration, and

Table 2: Comparison of the WT and P61A Denaturation Mechanism Using Various Denaturation Methods

	WT		P61A	
denaturation method	transition	mechanism	transition	mechanism
urea	single concentration dependent	$N_2 \leftrightarrows 2U$[a]	single but cooperativity (*m*-value) decreases as the concentration of FIS increases	$N_2 \leftrightarrows I_2 \leftrightarrows 2U$[b]
temperature	single concentration dependent	$N_2 \leftrightarrows 2U$	single but independent of FIS concentration (in the range of 10−90 °C, no urea, pH 7.4) and less cooperative than WT	$N_2 \leftrightarrows I_2 \leftrightarrows 2U$
low pH	single concentration dependent	$N_2 \leftrightarrows 2U$	no transition	N/A
temperature + urea	single concentration dependent	$N_2 \leftrightarrows 2U$	single concentration dependent but less cooperative than WT	$N_2 \leftrightarrows I_2 \leftrightarrows 2U$, urea destabilizes the intermediate
temperature at pH 3.5	single concentration dependent	$N_2 \leftrightarrows 2U$	biphasic with only the second transition being concentration dependent	$N_2 \leftrightarrows I_2 \leftrightarrows 2U$

[a] See ref *6*. [b] See ref *10*.

global fitting of the data was consistent with a three-state denaturation mechanism involving a dimeric intermediate (*10*). On the basis of the predominantly intramolecular interactions of the C-terminus of FIS (helices C and D, Figure 1) and the increased proteolytic susceptibility of this region in P61A FIS, we proposed that this dimeric intermediate comprised predominantly the dimeric core (helices A and B) with a disrupted C-terminus. It seems that the dimeric intermediate populated in the thermal denaturation studies shown here may involve an analogous intermediate. This is consistent with the agreement between the stabilities (ΔG) and *m*-values obtained for the denaturation of the urea-induced dimeric intermediates ($I_2 \leftrightarrows 2U$) detected at 20 °C ($\Delta G = 12.5$ kcal/mol, *m*-value $= 1.1 \pm 0.1$ kcal·mol^{-1}·M^{-1}) (*10*) and 90 °C ($\Delta G = 11.6$ kcal/mol, *m*-value $= 1.4 \pm 0.2$ kcal·mol^{-1}·M^{-1}) (Figure 5). It is noteworthy that the denaturation transition of P61A FIS at 90 °C (Figure 5) is cooperative, indicating that the dimeric intermediate retains a structured, solvent-protected, hydrophobic core, as opposed to a molten globule structure (*20*).

The thermal denaturation experiment of P61A FIS at low pH further suggests that the dimeric intermediate involves a disrupted C-terminus. At pH 3.5, P61A FIS exhibits a biphasic thermal denaturation transition (Figure 6B), with a first transition that overlays the early part of the WT transition and a second transition that seems less affected by pH, overlaying with the latter part of the P61A FIS transition at pH 7. Therefore, it appears that by decreasing the pH we were able to decouple the two transitions, $N_2 \leftrightarrows I_2$ and $I_2 \leftrightarrows 2U$, of P61A FIS. The pH dependence and concentration independence of the first transition (Figure 6B) indicate that it involves the unfolding of structure partially stabilized by aspartic and glutamic acid residues in intramolecular interactions. These characteristics describe the C-terminus of FIS, which contains the intramolecular salt bridges Glu 52−Lys 94 and Glu 59−Lys 91. Mutational studies suggest that these salt bridges are part of an electrostatic network that plays an important role in the stability and flexibility of the C-terminus of FIS (ref *8* and unpublished results). The second transition observed in the thermal denaturation of P61A FIS at pH 3.5 is concentration dependent and is much less sensitive to pH, as it matches the latter part of the thermal denaturation transition seen at pH 7. Thus, on the basis of the similar ΔG and *m*-values of the intermediates populated by urea and thermal denaturation, and the pH sensitivity of the thermal denaturation at low pH, we propose that the P61A FIS dimeric intermediate populated using various denaturation methods is the same and involves a disrupted C-terminus. This conclusion fits well with the fact that the C-terminal DNA-binding subdomain is largely composed of intramolecular interactions.

Structural Basis for the Increased Thermostability of P61A FIS. The high degree of similarity between the P61A and WT FIS crystal structures (*7*) [RMS deviation of 0.62 Å based on DeepView/Swiss-PDB viewer 3.7 (*21*)] indicates that the stabilization caused by the P61A mutation is not due to major changes to the native state structure. To understand the structural basis for the thermostability of P61A FIS, it is worth considering the factors involved in the stabilization of thermophilic proteins. The molecular basis of thermal stability has been investigated by comparing proteins from thermophilic organisms with their homologues from mesophiles (*22*, *23*), and significant differences have been determined, such as the ratio of polar to nonpolar residues (*22*), the number and environment of salt bridges (*24*, *25*), the degree of interdomain and intersubunit hydrophobic interactions (*26*−*28*), the number of hydrogen bonds (*29*), and backbone rigidity (*30*). Recently, Torrez et al. (*31*) have noted that small changes in protein sequence are capable of significantly increasing protein thermostability. Their computational methods using Poisson−Boltzmann electrostatics show that mutations that decrease repulsion or increase attraction of surface-charged groups commonly increase thermostability. In addition, Kumar et al. (*32*) determined, through a structural comparison of 18 pairs of mesophilic proteins with their thermophilic counterparts, that the main difference between the two was not the degree of packing, the ratio of polar to nonpolar surface area, the oligomeric state, or the hydrophobicity; rather, in most cases there was an increased number of side chain hydrogen bonds and salt bridges in the thermophilic proteins. The thermophiles were also shown to have more arginine and tyrosine residues and a lesser frequency of prolines in helices. Interestingly, FIS has four tyrosine residues, two of which (Tyr 51 and Tyr 95) form side chain hydrogen bonds with charged residues involved in the salt bridge network (*8*). Therefore, FIS appears to have inherent thermophilic properties that may be masked by the presence of Pro 61. Thus, the P61A mutation renders FIS with an additional thermostabilizing factor uncovered by Kumar et al. (*32*).

Although the P61A mutation was expected to stabilize FIS via stabilization of the helix in which it lies, it also may have enhanced the packing and rigidity of the native structure resulting in increased thermal stability. High structural rigidity is a common feature of thermostable proteins (*33*). In addition to better side chain packing, one thermodynamic consequence of structural rigidity is that the decreased conformational entropy of side chains reduces the entropic penalty for forming a salt bridge and, thus, results in their increased strength (*34*). Even though we lack direct evidence, the dramatic proteolytic resistance (*10*) of the P61A FIS A/B-helix dimer core is consistent with an increase in backbone rigidity, which may contribute to increase the stability of the intermolecular salt bridges (Arg 28−Glu 57 and Lys 32−Asp 64) between the A- and B-helices. Therefore, we are tempted to speculate that the intermolecular salt bridges may contribute significantly to the high temperature and low pH stability of P61A FIS. This conclusion is also supported by evidence from the crystal structure of P61A FIS that shows the formation of a previously nonexisting backbone hydrogen bond between Ala 61 and Glu 57, which is involved in one of the intermolecular salt bridges in FIS.

The observation that WT FIS, but not P61A FIS, undergoes acid-induced denaturation at 20 °C (Figure 6A) suggests that Glu 57 and Asp 64 may have a lower pK_a in P61A FIS. Alternatively, it may just be that the stabilizing [4 kcal/mol (*10*)] effect of the P61A mutation may allow FIS to overcome the potential destabilization caused by the protonation of the acidic residues at low pH. It is conceivable that the additional hydrogen bond of Glu 57 in P61A FIS, combined with an increase in rigidity that decreases the solvent exposure of the intermolecular salt bridges, may result in an abnormally low pK_a for Glu 57 and/or Asp 64. This assumption is

consistent with studies showing that acidic residues in proteins may experience a large shift in their pK_a (*35*, *36*). For example, the largely buried and hydrogen-bonded aspartic acids 83 and 101 in xylanase from *Bacillus circulans* were shown by ^{13}C nuclear magnetic resonance chemical shifts to have a pK_a less than 2 (*35*). Such a low pK_a was presumably made possible by hydrogen bond networks and side chain burial below the protein surface. Thus, the intermolecular salt bridges in P61A FIS may similarly have a lower pK_a, accounting for the stability to low pH and the persistence of the thermostable dimeric intermediate, even at pH 2. In future studies, we will mutate the residues involved in salt bridge interactions to probe whether the thermal stability of P61A FIS arises mainly by increasing the stability of the salt bridge interactions or rather by stabilizing the FIS structure such that its stability is much less dependent on the contribution of the salt bridges.

Implications for FIS Function and Stabilization. FIS is a highly regulated DNA-binding protein (*37*) that is involved in DNA inversion and has a regulatory effect on numerous *E. coli* genes. FIS expression is characteristically high early in the exponential growth phase and then drastically decreases in the cell afterward (*38*). Therefore, rapid degradation of FIS appears to be of functional significance. In our previous study we have shown that the P61A mutation results in a practically trypsin-resistant core (*10*), whereas the core of the WT protein is labile to proteolysis and, presumably, more easily degraded by the cell. The necessity for the cell to regulate FIS concentration may explain why proline 61 is 100% conserved among all types of enteric bacteria known to contain FIS (*8*, *39*). In this sense proline 61 may be an essential stability blocker. We suspect that the WT FIS has built into its structure many of the prerequisites for thermostability and that the proline at position 61 optimizes the function of FIS by modulating its thermostability and protease resistance.

In addition to the implications for function regulation mentioned above, a more stable FIS structure may be disfavored due to adverse structural effects. There is significant evidence suggesting that protein stabilization may often occur at the expense of structural specificity. Perhaps the best example of this effect has been demonstrated with the coiled-coil proteins, where changing an internal asparagine residue to a hydrophobic residue enhanced the stability of the peptide at the expense of oligomerization specificity (*40*−*42*). Based on the almost identical crystal structures of WT and P61A FIS (*7*) and the observation that the P61A mutation does not significantly decrease its activity or DNA binding (*7*), it appears that the structural specificity has not been compromised. In contrast, it is plausible that the presence of P61 may enhance the folding pathway specificity of FIS. In preliminary studies, we have observed that P61A FIS folds less efficiently than WT FIS due to protein misfolding (unpublished results). Evidence that proline residues may favor protein folding at the expense of stability has been observed for the DNA-binding protein of the yeast heat shock transcription factor (HSF) (*43*). Interestingly, this HSF protein also contains a strictly conserved proline residue that is at the center of a kinked helix. Mutation of this proline for other residues did not compromise function or the final structure but was shown to result in less soluble proteins due to alterations in the folding pathway (*43*). Thus, despite the price paid in terms of stability, it appears that proline residues may also be conserved in FIS and other proteins as a negative design strategy (*44*), not just to preserve structural specificity but also specificity of the folding pathway.

REFERENCES

1. Johnson, R. C., Bruist, M. F., and Simon, M. I. (1986) Host protein requirements for in vitro site-specific DNA inversion, *Cell 46*, 531−539.
2. Koch, C., and Kahmann, R. (1986) Purification and properties of the *Escherichia coli* host factor required for inversion of the G segment in bacteriophage Mu, *J. Biol. Chem. 261*, 15673−15678.
3. Ball, C. A., Osuna, R., Ferguson, K. C., and Johnson, R. C. (1992) Dramatic changes in Fis levels upon nutrient upshift in *Escherichia coli*, *J. Bacteriol. 174*, 8043−8056.
4. Xu, J., and Johnson, R. C. (1995) Identification of genes negatively regulated by Fis: Fis and RpoS comodulate growth-phase-dependent gene expression in *Escherichia coli*, *J. Bacteriol. 177*, 938−947.
5. Bruist, M. F., Glasgow, A. C., Johnson, R. C., and Simon, M. I. (1987) Fis binding to the recombinational enhancer of the Hin DNA inversion system, *Genes Dev. 1*, 762−772.
6. Hobart, S. A., Ilin, S., Moriarty, D. F., Osuna, R., and Colon, W. (2002) Equilibrium denaturation studies of the *E. coli* factor for inversion stimulation: implications for in vivo function, *Protein Sci. 11*, 1671−1680.
7. Yuan, H. S., Wang, S. S., Yang, W.-Z., Finkel, S. E., and Johnson, R. C. (1994) The structure of Fis mutant Pro^{61}Ala illustrates that the kink within the long α-helix is not due to the presence of the proline residue, *J. Biol. Chem. 269*, 28947−28954.
8. Boswell, S. A., Mathew, J., Beach, M., Osuna, R., and Colón, W. (2004) Variable contributions of tyrosine residues to the structural and spectroscopic properties of the factor for inversion stimulation, *Biochemistry 43*, 2964−2977.
9. Richardson, J. S., and Richardson, D. C. (1988) Amino acid preferences for specific locations at the ends of alpha helices, *Science 240*, 1648−1652.
10. Hobart, S. A., Meinhold, D. W., Osuna, R., and Colon, W. (2002) From two-state to three-state: Effect of P61A mutation on the dynamics and stability of the factor for inversion stimulation results in an altered equilibrium denaturation mechanism, *Biochemistry 41*, 13744−13754.
11. Park, Y. C., and Bedouelle, H. (1998) Dimeric tyrosyl-tRNA synthetase from *Bacillus stearothermophilus* unfolds through a monomeric intermediate. A quantitative analysis under equilibrium conditions, *J. Biol. Chem. 273*, 18052−18059.
12. Zolkiewski, M., Redowicz, M. J., Korn, E. D., Hammer, J. A., III, and Ginsburg, A. (1997) Two-state thermal unfolding of a long dimeric coiled-coil: the *Acanthamoeba* myosin II rod, *Biochemistry 36*, 7876−7883.
13. Steif, C., Weber, P., Hinz, H.-J., Flossdorf, J., Cesareni, G., and Kokkinidis, M. (1993) Subunit interaction provide a significant contribution to the stability of the dimeric four-alpha-helical-bundle protein ROP, *Biochemistry 32*, 3867−3876.
14. Kretschmar, M., and Jaenicke, R. (1999) Stability of a homodimeric Ca(2+)-binding member of the beta gamma-crystallin superfamily: DSC measurements on spherulin 3a from Physarum polycephalum, *J. Mol. Biol. 291*, 1147−1153.
15. Myers, J. K., Pace, C. N., and Scholtz, J. M. (1995) Denaturant m values and heat capacity changes: Relation to changes in accessible surface areas of protein unfolding, *Protein Sci. 4*, 2138−2148.
16. Soulages, J. L. (1998) Chemical denaturation: potential impact of undetected intermediates in the free energy of unfolding and m-values obtained from a two-state assumption, *Biophys. J. 75*, 484−492.
17. Swint, L., and Robertson, A. D. (1993) Thermodynamics of unfolding for turkey ovomucoid third domain: thermal and chemical denaturation, *Protein Sci. 2*, 2037−2049.
18. Kuroda, Y., Kidokoro, S., and Wada, A. (1992) Thermodynamic characterization of cytochrome *c* at low pH, *J. Mol. Biol. 223*, 1139−1153.
19. Nishii, I., Kataoka, M., and Goto, Y. (1995) Thermodynamic stability of the molten globule states of apomyoglobin, *J. Mol. Biol. 250*, 223−238.

20. Haynie, D. T., and Freire, E. (1993) Structural energetics of the molten globule state, *Proteins: Struct., Funct., Genet. 16*, 115−140.
21. Guex, N., and Peitsch, M. C. (1997) SWISS-MODEL and the Swiss-PdbViewer: an environment for comparative protein modeling, *Electrophoresis 18*, 2714−2723.
22. Suhre, K., and Claverie, J. M. (2003) Genomic correlates of hyperthermostability, an update, *J. Biol. Chem. 278*, 17198−17202.
23. Chakravarty, S., and Varadarajan, R. (2002) Elucidation of factors responsible for enhanced thermal stability of proteins: a structural genomics study, *Biochemistry 41*, 8152−8161.
24. Vetriani, C., Maeder, D. L., Tolliday, N., Yip, K. S., Stillman, T. J., Britton, K. L., Rice, D. W., Klump, H. H., and Robb, F. T. (1998) Protein thermostability above 100 °C: a key role for ionic interactions, *Proc. Natl. Acad. Sci. U.S.A. 95*, 12300−12305.
25. Merz, A., Knochel, T., Jansonius, J. N., and Kirschner, K. (1999) The hyperthermostable indoleglycerol phosphate synthase from *Thermotoga maritima* is destabilized by mutational disruption of two solvent-exposed salt bridges, *J. Mol. Biol. 288*, 753−763.
26. Biro, J., Fabry, S., Dietmaier, W., Bogedain, C., and Hensel, R. (1990) Engineering thermostability in archaebacterial glyceraldehyde-3-phosphate dehydrogenase. Hints for the important role of interdomain contacts in stabilizing protein conformation, *FEBS Lett. 275*, 130−134.
27. Kirino, H., Aoki, M., Aoshima, M., Hayashi, Y., Ohba, M., Yamagishi, A., Wakagi, T., and Oshima, T. (1994) Hydrophobic interaction at the subunit interface contributes to the thermostability of 3-isopropylmalate dehydrogenase from an extreme thermophile, *Thermus thermophilus*, *Eur. J. Biochem. 220*, 275−281.
28. Toth-Zsamboki, E., Oury, C., Watanabe, H., Nilius, B., Vermylen, J., and Hoylaerts, M. F. (2002) The intracellular tyrosine residues of the ATP-gated P2X1 ion channel are essential for its function, *FEBS Lett. 524*, 15−19.
29. Zhou, H. X. (2002) Towards the physical basis of thermophilic proteins: linking of enriched polar interactions and reduced heat capacity of unfolding, *Biophys. J. 83*, 3126−3133.
30. Hardy, F., Vriend, G., van der Vinne, B., Frigerio, F., Grandi, G., Venema, G., and Eijsink, V. G. (1994) The effect of engineering surface loops on the thermal stability of *Bacillus subtilis* neutral protease, *Protein Eng. 7*, 425−430.
31. Torrez, M., Schultehenrich, M., and Livesay, D. R. (2003) Conferring thermostability to mesophilic proteins through optimized electrostatic surfaces, *Biophys. J. 85*, 2845−2853.
32. Kumar, S., Tsai, C. J., and Nussinov, R. (2000) Factors enhancing protein thermostability, *Protein Eng. 13*, 179−191.
33. Jaenicke, R. (2000) Do ultrastable proteins from hyperthermophiles have high or low conformational rigidity?, *Proc. Natl. Acad. Sci. U.S.A. 97*, 2962−2964.
34. Thomas, A. S., and Elcock, A. H. (2004) Molecular simulations suggest protein salt bridges are uniquely suited to life at high temperatures, *J. Am. Chem. Soc. 126*, 2208−2214.
35. Joshi, M. D., Hedberg, A., and McIntosh, L. P. (1997) Complete measurement of the pK_a values of the carboxyl and imidazole groups in *Bacillus circulans* xylanase, *Protein Sci. 6*, 2667−2670.
36. Georgescu, R. E., Alexov, E. G., and Gunner, M. R. (2002) Combining conformational flexibility and continuum electrostatics for calculating p*K*(a)s in proteins, *Biophys. J. 83*, 1731−1748.
37. Finkel, S. E., and Johnson, R. C. (1992) The Fis Protein: it's not just for DNA inversion anymore, *Mol. Microbiol. 6*, 3257−3265.
38. Ali Azam, T., Iwata, A., Nishimura, A., Ueda, S., and Ishihama, A. (1999) Growth phase-dependent variation in protein composition of the *Escherichia coli* nucleoid, *J. Bacteriol. 181*, 6361−6370.
39. Beach, M. B., and Osuna, R. (1998) Identification and characterization of the fis operon in enteric bacteria, *J. Bacteriol. 180*, 5932−5946.
40. Harbury, P. B., Zhang, T., Kim, P. S., and Alber, T. (1993) A switch between two-, three-, and four-stranded coiled coils in GCN4 leucine zipper mutants, *Science 262*, 1401−1407.
41. Potekhin, S. A., Medvedkin, V. N., Kashparov, I. A., and Venyaminov, S. (1994) Synthesis and properties of the peptide corresponding to the mutant form of the leucine zipper of the transcriptional activator GCN4 from yeast, *Protein Eng. 7*, 1097−1101.
42. Lumb, K. J., and Kim, P. S. (1995) A buried polar interaction imparts structural uniqueness in a designed heterodimeric coiled coil, *Biochemistry 34*, 8642−8648.
43. Hardy, J. A., and Nelson, H. C. (2000) Proline in alpha-helical kink is required for folding kinetics but not for kinked structure, function, or stability of heat shock transcription factor, *Protein Sci. 9*, 2128−2141.
44. Richardson, J. S., and Richardson, D. C. (2002) Natural beta-sheet proteins use negative design to avoid edge-to-edge aggregation, *Proc. Natl. Acad. Sci. U.S.A. 99*, 2754−2759.

BI050640K